Published November 14, 2005

Avidity for antigen shapes clonal dominance in CD8+ T cell populations specific for persistent DNA viruses

David A. Price,[1] Jason M. Brenchley,[1] Laura E. Ruff,[1] Michael R. Betts,[2] Brenna J. Hill,[1] Mario Roederer,[3] Richard A. Koup,[2] Steven A. Migueles,[4] Emma Gostick,[5] Linda Wooldridge,[5] Andrew K. Sewell,[5] Mark Connors,[4] and Daniel C. Douek[1]

[1]Human Immunology Section, [2]Immunology Laboratory, [3] Immunotechnology Section, Vaccine Research Center, and [4]Laboratory of Immunoregulation, National Institute of Allergy and Infectious Diseases, National Institutes of Health, Bethesda, MD 20892

[5]Nuffield Department of Clinical Medicine, University of Oxford, John Radcliffe Hospital, Oxford OX3 9DU, England, UK

The forces that govern clonal selection during the genesis and maintenance of specific T cell responses are complex, but amenable to decryption by interrogation of constituent clonotypes within the antigen-experienced T cell pools. Here, we used point-mutated peptide–major histocompatibility complex class I (pMHCI) antigens, unbiased *TCRB* gene usage analysis, and polychromatic flow cytometry to probe directly ex vivo the clonal architecture of antigen-specific CD8+ T cell populations under conditions of persistent exposure to structurally stable virus-derived epitopes. During chronic infection with cytomegalovirus and Epstein-Barr virus, CD8+ T cell responses to immunodominant viral antigens were oligoclonal, highly skewed, and exhibited diverse clonotypic configurations; TCRB CDR3 sequence analysis indicated positive selection at the protein level. Dominant clonotypes demonstrated high intrinsic antigen avidity, defined strictly as a physical parameter, and were preferentially driven toward terminal differentiation in phenotypically heterogeneous populations. In contrast, subdominant clonotypes were characterized by lower intrinsic avidities and proportionately greater dependency on the pMHCI–CD8 interaction for antigen uptake and functional sensitivity. These findings provide evidence that interclonal competition for antigen operates in human T cell populations, while preferential CD8 coreceptor compensation mitigates this process to maintain clonotypic diversity. Vaccine strategies that reconstruct these biological processes could generate T cell populations that mediate optimal delivery of antiviral effector function.

CORRESPONDENCE
David A. Price:
davidprice@nih.gov
OR
Daniel C. Douek:
ddouek@nih.gov

Abbreviations used: pMHC, peptide-MHC; pMHCI, pMHC class I.

Competition for limited resources is a universal biological principle. In the case of adaptive immunity, it is established that humoral responses are governed by Darwinian laws through antigen-mediated positive selection of cognate antibodies from a naturally generated diverse peripheral repertoire with subsequent affinity maturation. For T cell responses, the situation is less clear. The TCR antigen recognition system operates within a substantially lower range of affinities and exhibits distinct kinetics compared with antibody–antigen interactions (1). Despite this, evidence from experimental manipulations in murine models suggests that competitive effects can influence T cell responses to both identical and different peptide-MHC (pMHC) antigens (2). These processes appear to operate at the level of the APC, and are thought to be governed by T cell avidity and precursor frequency (2–16). However, it is uncertain whether, and under what conditions, such processes operate in the human immune system.

CMV and EBV establish lifelong infection in human hosts. The control of viral replication in this persistent state is dependent on functional CD8+ T cell immunity (17). Several features of the host–pathogen relationship during infection with these herpesviruses are relevant to the issue of interclonal competition within specific T cell populations. First, the provision of a persistent antigenic stimulus is an essential requirement for progressive evolution of the cognate T cell response. In contrast with transient perturba-

The online version of this article contains supplemental material.

Supplemental Material can be found at:
http://jem.rupress.org/content/suppl/2005/11/14/jem.20051357.DC1.html

Published November 14, 2005

JEM

A

ID	TCRBV	CDR3	TCRBJ	%freq
F	6-5	CASSYSTGTPGIYT	1.2	85
12.1%	27	CASTPAGGAPGELF	2.2	15
R	7-6	CASSLAPGATNEKLF	1.4	91
5.11%	27	CASSFSGGAPGELF	2.2	5
	6-5	CASSYFGGNTEAF	1.1	2
	7-6	CASSLAPGATSEKLF	1.4	2
H	6-5	CASSYQTGTIYGYT	1.2	41
4.76%	6-5	CASSPQTGAIYGYT	1.2	14
	9	CASSALGGGGTGELF	2.2	13
	30	CAWIPGTGGAGGL	2.3	9
	6-5	CASSPVQGAFYNSPLH	1.6	7
	20-1	CSARDFDRTGELF	2.2	6
	29-1	CSVDETGGGETQY	2.5	6
	7-6	CASSLAPGATNEKLF	1.4	3
	6-5	CASSYQTGAIYGYT	1.2	1
D	7-6	CASSLAPGTTNEKLF	1.4	62
3.7%	6-5	CASSSLYGDTGELF	2.2	10
	27	CASSLVSGSPTGELF	2.2	10
	6-5	CASSYATGIGNYGYT	1.2	9
	12-4	CASSSVTEAF	1.1	3
	27	CASSFGTGHTGELF	2.2	3
	6-5	CANSYATGIGNYGYT	1.2	1
	6-5	CASSYFGSQSEQY	2.7	1
N	27	CASNPSGGYTGELF	2.2	80
1.99%	6-5	CASSLTTGTGSYGYT	1.2	10
	6-5	CASSLQTGVRSYEQY	2.7	4
	27	CASSLEGYTEAF	1.1	3
	12-4	CASSFWREPTYEQY	2.7	2
	4-1	CASSQADRAVYGYT	1.2	1
	12-4	CASSSANYGYT	1.2	1
K	12-4	CASSSANYGYT	1.2	70
1.43%	12-4	CASSSAHYGYT	1.2	16
	27	CASSLLIQGGENTEAF	1.1	5
	28	CASSVQGYTEAF	1.1	5
	12-4	CASSPGSINYGYT	1.2	3
M	12-4	CASSSAYYGYT	1.2	28
1.35%	10-2	CASSESMIQH	1.5	27
	18	CASSPRQGGKQPQH	1.5	8
	13	CASHYGGSSYEQY	2.7	7
	30	CAWSVSDIMNTEAF	1.1	7
	7-2	CASSTPWGGTSGATDTQY	2.3	3
	12-4	CASSFFSKKYNNEQF	2.1	3
	27	CASSLEGFTEAF	1.1	3
	7-8	CASSLSPTSGLSYEQY	2.7	2
	7-8	CASSLGGGGFYEQY	2.7	2
	12-4	CASSVVNEQF	2.1	2
	12-4	CASSLVGGRYGYT	1.2	2
	15	CATSRDLVAETQY	2.7	2
	20-1	CSARDPLDYVRTDTQY	2.3	2
	27	CASSWLMGTTYNEQF	2.1	2
	29-1	CSVDRYGGDTYEQY	2.7	2
P	29-1	CSVGGTLDTQY	2.3	92
0.64%	6-1	CASSEVGATNYGYT	1.2	3
	6-2/3	CASSYFPLADTQY	2.3	3
	27	CASSLEGYTEAF	1.1	2
S	13	CASSSLGGAGTGELF	2.2	60
0.21%	12-4	CASSSANYGYT	1.2	24
	27	CASSRPGQGGYEQY	2.7	11
	27	CASSFAGGAAGELF	2.2	3
	27	CASSPGTGHGELF	2.2	1
	28	CASSFGLNQPQH	1.5	1

B

ID	TCRBV	CDR3	TCRBJ	%freq
T	20-1	CSARDRSLGNTIY	1.3	46
1.8%	25-1	CASSTSDTQY	2.3	28
	4-1	CASSHVGGYEQY	2.7	9
	6-2/3	CASSLGNTEAF	1.1	5
	18	CASSPLAGKGEPQH	1.5	4
	20-1	CSARGQGRDAAF	1.1	4
	2	CASSAWLVETQY	2.5	2
	7-8	CASSQEEANYGYT	1.2	2
	29-1	CSVEDQRKTKNIQY	2.4	2
F	29-1	CSTQEGGYGYT	1.2	81
0.5%	2	CASSEGRVLPGELF	2.2	5
	20-1	CSARDRTGNGYT	1.2	5
	20-1	CSARDGTGNGYT	1.2	4
	2	CASSEGRVSPGELF	2.2	1
	2	CASSEGRVAPGELF	2.2	1
	20-1	CSAEPGTQGGTQY	2.5	1
	29-1	CSVGTGGTNEKLF	1.4	1
P	20-1	CSARDQTGNGYT	1.2	92
0.4%	29-1	CSSQEGGYGYT	1.2	6
	20-1	CSARDQTGNDYT	1.2	1
B	20-1	CSARDGTGNGYT	1.2	59
0.39%	29-1	CSVPFEGGTLETQY	2.5	15
	7-8	CASTPDGDNEQF	2.1	4
	20-1	CSARDGTGNDYT	1.2	4
	20-1	CSARIGVGNTIY	1.3	4
	3-1	CASSQDRQGQIYGYT	1.2	2
	20-1	CSAREGTGNGYT	1.2	2
	20-1	CSARIGVGNAIY	1.3	2
	20-1	CSARVGVGNTIY	1.3	2
	29-1	CSSQEGGYGYT	1.2	2
	29-1	CSVPFEGGTLETQH	2.5	2
M	12-4	CASSFGQQETQY	2.5	48
0.22%	9	CASSVAGGDEQY	2.7	21
	5-1	CASSFSRDSDEQF	2.1	19
	20-1	CSARDNLSGYT	1.2	4
	20-1	CSARDGTGNGYT	1.2	3
	29-1	CSATVTGGWNEQF	2.1	3
	5-1	CASSFSRNSDEQF	2.1	1
	6	CASSLDLGTAKYGYT	1.2	1

C

ID	Sequence alignment
CMV	C A S S L E G Y T E A F
N	tgtgccagcagtttagagggttacactgaagctt
P	----------cc-c-----g----------
CMV	C A S S S A N Y G Y T
N	tgtgccagcagttctgctaactatggctaca
K	----------c--a----------
S	----------c----------
CMV	C A S S L A P G A T N E K L
H	tgtgccagcagcttagcgcccggggctacaaatgaaaaac
R	----------t-----a-t----------
EBV	C S S Q E G G Y G Y T
P	tgcagctctcaggaaggggggc tatggctacacct
B	------agc-----g-c----------
EBV	C S A R D G T G N G Y T
F	tgcagtgctagagatggaacagggaatggctacacc
B	----------g----------
M	----------g--c----------

Figure 1. Clonal analysis of CD8⁺ T cells specific for CMV NV9 and EBV GL9. (A) CD8⁺ T cells specific for CMV NV9. TCRBV usage, CDR3 amino acid sequence and percent frequency, and TCRBJ usage are shown for each clonotype defined by its CDR3. Sequences with identical amino acid residues are shown in color. The percent frequency of CD8⁺ T cells that bound cognate pMHCI wild-type tetramer is shown below the identifier letter code (ID) for each donor. (B) CD8⁺ T cells specific for EBV GL9. Details as for A. (C) CDR3 codon usage of CMV- and EBV-specific CD8⁺ T cell clonotypes that have the same CDR3 amino acid sequence between different donors. Each section defines a CDR3 amino acid sequence and, below that, the CDR3 nucleotide alignments of all constituent clonotypes. Colors correspond to those in A and B.

Published November 14, 2005

tions, continuous exposure to antigen theoretically favors maturation of the T cell response while allowing equilibration of kinetic effects due to differences in clonotype precursor frequency (4, 11). Second, persistent infection is characterized by viral latency. In addition, multiple mechanisms exist to minimize the presentation of pMHC class I (pMHCI) antigen on the surface of the infected cell. Antigen load is therefore relatively low, and evidence of competition for this limited resource should become most apparent under these conditions. Third, the double-stranded DNA genomes of herpesviruses are genetically stable. Thus, in contrast with RNA viruses, the fundamental biology of adaptive immunity is not obscured by the myriad effects of antigenic mutation. Fourth, immunodominant $CD8^+$ T cell responses to these pathogens are generated at typically high frequencies; this condition is likely to be an essential requirement for the observation of interclonal competition (11). In light of these considerations, we reasoned that chronic infections with CMV and EBV might represent the ideal human system in which to seek evidence for competitive effects in vivo; we therefore examined the properties of individual clonotypes specific for immunodominant pMHCI antigens derived from these viruses to illuminate the factors that shape clonal selection in the periphery under these conditions.

RESULTS

Clonal structure of $CD8^+$ T cell populations specific for CMV and EBV

Immunodominant HLA A*0201-restricted $CD8^+$ T cells specific for CMV $pp65_{495\text{-}503}$ (NV9 from hereon) and EBV $BMLFI_{259\text{-}267}$ (GL9 from hereon) were identified directly ex vivo with cognate fluorescent pMHCI tetramers and sorted by flow cytometry. A template-switch anchored RT-PCR was used to amplify all expressed *TCRB* gene products without bias (18); at least 50 subcloned PCR products were sequenced for each isolated antigen-specific $CD8^+$ T cell population. The amino acid sequences spanning the expressed CDR3s formed at the TCRB VDJ junctional region and the frequency of each response within the $CD8^+$ T cell population are shown for all 11 donors in Fig. 1 (A and B).

Three consistent features emerged from this analysis. First, $CD8^+$ T cell responses to CMV NV9 and EBV GL9 were oligoclonal in the setting of chronic infection. Second, a clear hierarchical structure was apparent in most cases, with one or two clonotypes dominating the antigen-specific T cell population. Third, in contrast with the restricted TCR usage that characterizes responses to some immunodominant pMHCI antigens (19–21), both the CMV NV9 and EBV GL9 epitope-specific $CD8^+$ T cell populations exhibited substantial clonotypic diversity. However, although no consensus TCRB CDR3 motifs were identified, several themes transpired that presumably reflect distinct modes of antigen recognition. For example, TCRBV12-4 was associated with TCRBJ1.2 and conserved usage of a serine residue at CDR3 position 4 in several clonotypes specific for CMV NV9; interestingly, this 4S residue replaced the germline-encoded leucine. Similarly, CMV NV9 was commonly recognized by clontoypes expressing TCRBV6-5/TCRBJ1.2, with threonine/glycine at CDR3 positions 6/7 respectively and a preferred hydrophobic residue at position 4 (Fig. 1). Dominant $CD8^+$ T cell clonotypes specific for EBV GL9 were frequently characterized by TCRBV20-1 linked to a nongermline aspartate residue at CDR3 position 4 (Fig. 1); similar themes were identified in an earlier study (22). Importantly, these observations are representative of the in vivo situation in peripheral blood, because no manipulation of virus-specific $CD8^+$ T cells was undertaken in vitro.

The following observations are also noteworthy: (a) no significant correlations were detected between the magnitude of the antigen-specific $CD8^+$ T cell population and the number of constituent clonotypes ($P = 0.08$; Spearman's Rank); (b) no consistent features at the level of primary sequence were found that distinguished dominant from subdominant clonotypes; and (c) HIV coinfection in chronic phase did not appear to affect the clonal structure of $CD8^+$ T cell responses to CMV NV9 and EBV GL9.

Evidence for TCR-mediated clonal selection

Closer inspection of the data presented in Fig. 1 (A and B) revealed that public clonotypes bearing identical TCRB CDR3 amino acid sequences were present in several donors. These promiscuous CDR3s were encoded by distinct nucleotide sequences in each case and confined to individual antigen-specific $CD8^+$ T cell populations (Fig. 1 C). Furthermore, in some instances, dominant TCRB CDR3s within the same donor were encoded distinctly (unpublished data). Together with the presence of characteristic themes within the private repertoire at the level of primary TCRB CDR3 structure, these observations provide indirect evidence for antigen-driven clonal selection mediated through the TCR. In some cases, this was further substantiated by N-encoded CDR3 residue conservation; for example, the serine/glutamine sequence at the V–D junction is nongermline in both public TCRBV29-1 clonotypes specific for EBV GL9 (Fig. 1 C). To extend these findings and clarify the nature of the selection process, we studied the properties of constituent clonotypes within these CMV- and EBV-specific $CD8^+$ T cell responses.

Assessment of $CD8^+$ T cell avidity using point-mutated soluble pMHCI antigens

The extent to which a $CD8^+$ T cell depends on the pMHCI–CD8 interaction for stable pMHCI tetramer binding is a measure of intrinsic avidity for antigen and likely reflects, in a nonlinear manner, both the affinity with which TCR binds cognate pMHCI ligand and other factors such as the distribution, density, and mobility of TCR in the cell membrane. Thus, $CD8^+$ T cells with high intrinsic avidity for a defined antigen can be selectively identified using pMHCI tetramers with mutations in the $\alpha 3$ domain that abrogate CD8 binding without affecting the

Published November 14, 2005

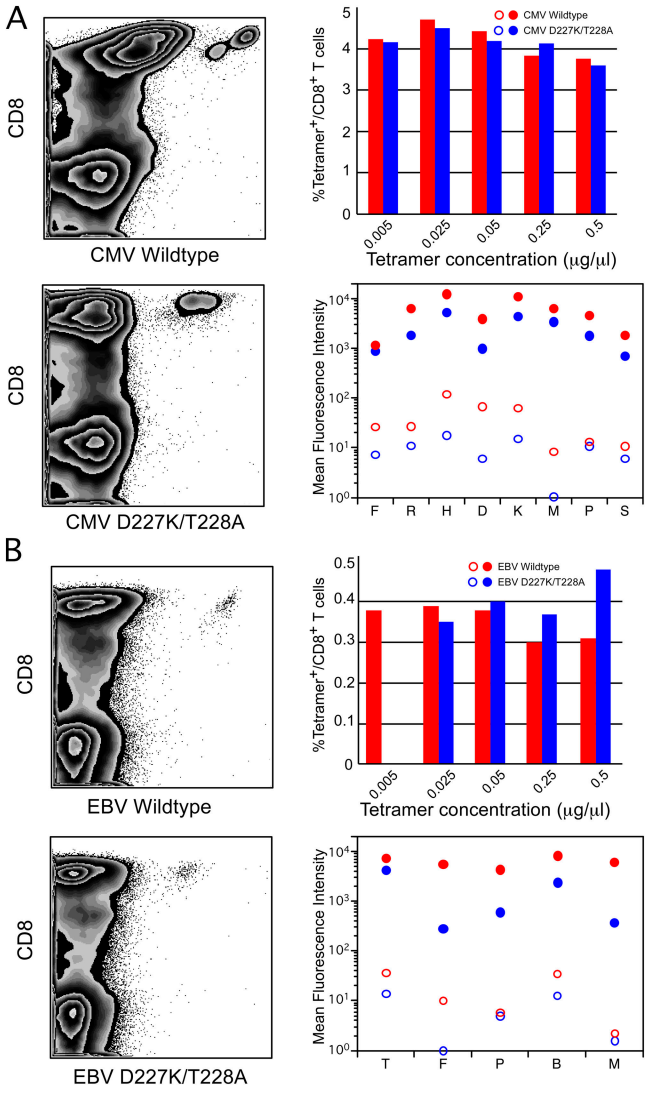

Figure 2. Wild-type and CD8-null pMHCI tetramers stain comparable populations of HLA A*0201-restricted CMV- and EBV-specific CD8+ T cells directly ex vivo. Representative tetramer staining patterns and titrations are shown for: (A) donor D (specificity: CMV NV9) and (B) donor B (specificity: EBV GL9). Data plots represent live, $CD3^+$ lymphocytes. (A and B, bottom right) The mean fluorescence intensity (MFI) of staining with both the wild-type (red) and CD8-null (blue) tetramers at a concentration of 0.5 μg/μl for both cognate ($CD8^+tet^+$; closed circles) and noncognate ($CD8^+tet^-$; open circles) binding is shown for all donors tested. In each case, the MFI values are internally comparable. The p-values derived from nonparametric paired *t* test comparisons of the MFIs for wild-type and CD8-null tetramer binding across all donors shown were as follows: CMV NV9 cognate, 0.078; CMV NV9 noncognate, 0.078; EBV GL9 cognate, 0.0009; and EBV GL9 noncognate, 0.0625.

integrity of the TCR interaction (23, 24). Intrinsic avidity is likely to be a closer reflection of TCR/pMHCI affinity than "coreceptor-compensated" avidity; from here on, the term avidity refers to the former parameter unless otherwise stated.

In 8/8 donors studied, both wild-type and CD8-null CMV NV9 tetramers identified cognate $CD8^+$ T cell populations of similar magnitude (Fig. 2 A and not depicted). Molecular analysis of these respective populations demonstrated the presence of identical constituent clonotypes at equivalent frequencies within donors ($n = 2$; unpublished data). Thus, $CD8^+$ T cell responses to CMV NV9 exhibit a high degree of avidity for cognate pMHCI antigen. Similarly, in 2/5 donors studied, both wild-type and CD8-null EBV GL9 tetramers identified cognate $CD8^+$ T cell populations of comparable magnitude and clonotypic composition (Fig. 2 B and not depicted).

The CD8-null pMHCI tetramers exhibited several interesting features in these experiments. First, background staining of $CD8^+$ T cells was substantially reduced (Fig. 2). This is consistent with previous studies using pMHCI tetramers with reduced, but measurable, CD8 binding properties (25). In addition, the intensity of cognate staining with the CD8-null reagents was consistently lower compared with the corresponding wild-type pMHCI tetramers under standardized conditions (Fig. 2). These findings indicate a role for CD8 in both cognate and noncognate antigen binding. Second, and in contrast with the corresponding wild-type reagent under identical conditions, CD8-null pMHCI tetramers failed to stain the cognate $CD8^+$ T cell population at lower concentrations in several donors (Fig. 2 B and not depicted). This observation indicates that the pMHCI–CD8 interaction assumes greater relevance at low concentrations of soluble ligand and presumably reflects a spectrum of avidities in antigen-specific $CD8^+$ T cell responses. Third, in 3/5 donors, the CD8-null reagent stained only a fraction of the $CD8^+$ T cell population specific for EBV GL9 compared with the corresponding wild-type tetramer even at high concentrations (Figs. 2 and 3; donor T, 0.74 vs. 1.8%; donor M, 0.11 vs. 0.22%; donor F, 0.4 vs. 0.5%). These subtle differences were exploited to separate antigen-specific $CD8^+$ T cell clonotypes according to avidity based on differential staining patterns with CD8-null pMHCI tetramers directly ex vivo.

Dissection of interclonal avidity relationships in $CD8^+$ T cell populations directly ex vivo

In donor T, the cognate CD8-null pMHCI tetramer identified a substantially smaller population of $CD8^+$ T cells specific for EBV GL9 than the corresponding wild-type tetramer across a range of concentrations (Fig. 3). Consistent with the relative clonal frequencies estimated by molecular methods, we reasoned that this high avidity population might comprise the dominant clonotype within the total antigen-specific $CD8^+$ T cell response (Fig. 1 B). Analysis of the constituent clonotypes confirmed this hypothesis (Fig. 3). Similarly, in donor F, the smaller EBV GL9-specific $CD8^+$ T cell population (0.4% of total) identified with the CD8-null tetramer contained 3/4 of the dominant clonotypes, but none of the subdominant clonotypes, that were present in the population detected using the corresponding wild-type reagent (Fig. 1 and not depicted). Thus, dominant clonotypes exhibit high avidity for cognate viral antigen.

Published November 14, 2005

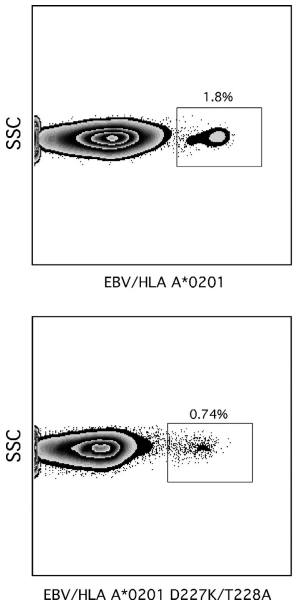

V	CDR3	J	Freq
20-1	CSARDRSLGNTIY	1.3	46
25-1	CASSTSDTQY	2.3	28
4-1	CASSHVGGYEQY	2.7	9
6-2	CASSLGNTEAF	1.1	5
18	CASSPLAGKGEPQH	1.5	4
20-1	CSARGQGRDAAF	1.1	4
2	CASSAWLVETQY	2.5	2
29-1	CSVEDQRKTKNIQY	2.4	2
7-8	CASSQEEANYGYT	1.2	2

V	CDR3	J	Freq
20-1	CSARDRSLGNTIY	1.3	96
7-8	CASSLERAMNTRFQPQH	1.5	1
11-2	CASSLEGGTDTQY	2.3	1
1	CASSVGASLNTEAF	1.1	1

Figure 3. Interclonal avidity differences can be separated directly ex vivo using wild-type and CD8-null pMHCI tetramers in parallel. $CD8^+$ T cells specific for EBV GL9 in PBMCs from donor T were stained with the corresponding wild-type (top) or CD8-null (bottom) pMHCI tetramers and sorted by flow cytometry. Constituent clonotypes within each sorted population are shown (right; total number of clones analyzed: wild-type, 65; CD8-null, 77). Common clonotypes were identical at the nucleotide level.

In donor F, both wild-type and CD8-null pMHCI tetramers identified comparable populations of $CD8^+$ T cells specific for CMV NV9 across a range of concentrations (Fig. 4 A); the clonotypic profile was identical in each case (Fig. 1 A and not depicted). However, a distinct staining pattern was observed in titration experiments with the CD8-null reagent. A subpopulation of antigen-specific T cells, characterized by low intensity staining with tetramer and high levels of CD8 coreceptor expression, became progressively more prominent at lower concentrations (Fig. 4 A). Previous work has shown that cognate $CD8^+$ T cells internalize pMHCI tetramers at 37°C (26). In this light, we reasoned that the titration experiment represented an ex vivo competition assay in which clonotypes of lower relative avidity are exposed at limiting concentrations of antigen in the absence of a pMHCI–CD8 interaction. The latter could potentially compensate under physiological circumstances for a low affinity TCR–pMHCI interaction (27–29), and the cosegregation of high CD8 expression levels with reduced uptake of the tetramer lends credence to this hypothesis (Fig. 4 A). Fine resolution flow cytometric sorting and molecular analysis confirmed that the distinct subpopulation isolated on the basis of reduced intensity staining with the cognate CD8-null reagent comprised predominantly the subdominant clonotype (Fig. 4 B). Parallel studies of *TCRA* gene usage identified only two mRNA species (unpublished data), thereby indicating that the incomplete segregation patterns were more likely reflective of technical parameters, which were set to capture the outcompeted population with maximal visual resolution and distinction from background. The minority clonotype in this subpopulation was not present in the analysis presented for donor F in Fig. 1 A, but was identified at very low frequencies in similar analyses from another time point; the relative enrichment and exclusive appearance of this clonotype within the "low avidity" compartment is consistent with the hypothesis that competition for antigen is a determinant of clonal hierarchy. No such distinction in terms of clonotypic composition was observed between populations separated according to intensity of staining with the corresponding wild-type tetramer, presumably because the interclonal compensated avidities approximate each other (unpublished data). Comparable experiments were performed with the CD8-null pMHCI tetramer using PBMCs from donors K and P; in each case, the subdominant clonotypes specific for CMV NV9 were substantially more prevalent in the T cell populations sorted on the basis of lower intensity staining, despite the relative lack of distinct staining patterns compared with donor F (Fig. 4 C). As observed before (Fig. 4 B), additional clonotypes were detected only within the population that exhibited low avidity for cognate antigen; the finding that even the least prevalent of these clonotypes exhibited *TCRB* gene usage patterns characteristic of the "themes" observed for $CD8^+$ T cells that recognize CMV NV9 attests to their specificity and argues against contamination with noncognate clonotypes (Figs. 1 and 4 C). Thus, subdominant clonotypes are distinguished by lower relative avidities for cognate pMHCI and a consequently greater dependence on CD8 for soluble antigen uptake.

The role of CD8 in transduction from antigen avidity to functional sensitivity

To examine the relationship between effector function and antigen avidity directly ex vivo, C1R cells were generated that expressed equivalent levels of either wild-type or CD8-null HLA A*0201 tagged with GFP. These cells were pulsed in parallel with exogenous CMV NV9 peptide at a range of concentrations and used to present antigen to PBMCs from donor F. In conjunction with a flow cytometric readout based on functional parameters, this approach enabled the discrimination of interclonal avidity and antigen sensitivity relationships formally both in the presence and absence of a pMHCI–CD8 interaction. Substantial differences in functional sensitivity were observed according to the nature of the peptide-presenting cell; for C1R cells bearing mutant CD8-null HLA A*0201, the peptide concentration threshold for detection of cytokine release in the dominant responding $CD8^+$ T cell clonotype was two orders of magnitude higher than that observed for the corresponding C1R cells expressing wild-type HLA A*0201 (Fig. 5 A). This is consistent with a predominant role for CD8 at low levels of antigen density during the process of T cell activation (30). Higher antigen concentrations were also required to elicit functional responses in the subdominant TCRVβ27 clonotype com-

Published November 14, 2005

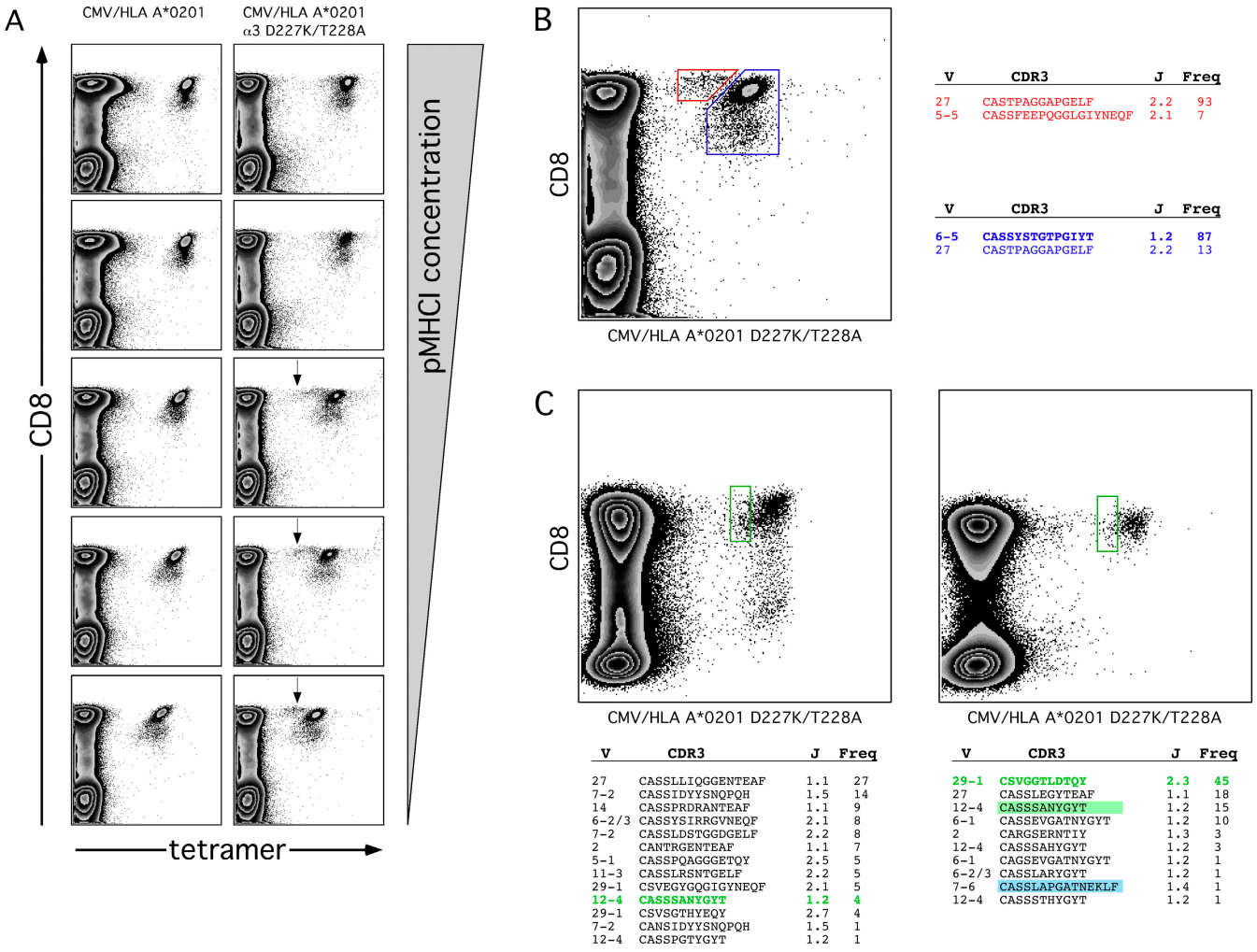

Figure 4. Differential patterns of staining with CD8-null pMHCI tetramers can distinguish subtle variations in clonotype avidity directly ex vivo. (A) Titration experiments with PBMCs from donor F reveal a distinct subpopulation of CD8$^+$ T cells specific for CMV NV9 (indicated by arrow) that is out-competed for uptake of cognate CD8-null pMHCI tetramer at low concentrations (right); this staining pattern is not observed with the corresponding wild-type pMHCI tetramer (left). Concentrations of each pMHCI tetramer, from top to bottom, are: 0.5, 0.25, 0.05, 0.025, and 0.005 μg/μl. Plots are gated on live lymphocytes. (B) The subdominant clonotype specific for CMV NV9 from donor F is identified by reduced intensity staining with the corresponding CD8-null pMHCI tetramer at low concentrations. Subpopulations of cognate CD8$^+$ T cells were sorted by flow cytometry through gates depicted by the colored boxes (left). Constituent clonotypes within each sorted population are shown (right; total number of clones analyzed: CD8-null bright, 83; CD8-null dim, 87). The dominant clonotype identified with the corresponding wild-type tetramer (Fig. 1) is shown in bold. Common clonotypes were identical at the nucleotide level. (C) Donor K (left) and donor P (right) PBMCs were stained with the CD8-null CMV NV9 pMHCI tetramer and sorted through the gates indicated by the colored boxes. Clonotypes identified by molecular analysis of these sorted cells are shown below each panel (total number of clones analyzed: donor K, 74; donor P, 67). Clonal representation and dominance hierarchies from parallel sorts of CD8$^+$ T cells that stained brightly with the CD8-null reagent reflected those identified with the corresponding wild-type tetramer in each case (Fig. 1 and not depicted); the dominant clonotypes from these sorts are in bold. In donor P, public clonotypes were detected within the gated CD8$^+$ T cell population; these are shown in colored boxes that match those in Fig. 1 C.

pared with the dominant clonotype; this distinction was exaggerated in the absence of a pMHCI–CD8 interaction, and reflected by interclonal differences in TCR down-regulation under these conditions (Fig. 5 A). Comparable results were obtained with PBMCs from donor T using exogenous EBV GL9 peptide in this system, although the antigen density threshold required for functional activation was substantially higher (Fig. 5 B). Interestingly, the subdominant TCRVβ25-1 clonotype exhibited minimal TCR down-regulation, even in the presence of pMHCI–CD8 binding (Fig. 5 B). This observation is consistent with the lower avidity of this clonotype identified by lack of staining with the cognate CD8-null tetramer (Fig. 3), and suggests a complex relationship between TCR triggering and downstream functional consequences.

The observed interclonal cosegregation of avidity and TCR down-regulation suggests that competitive effects can

Published November 14, 2005

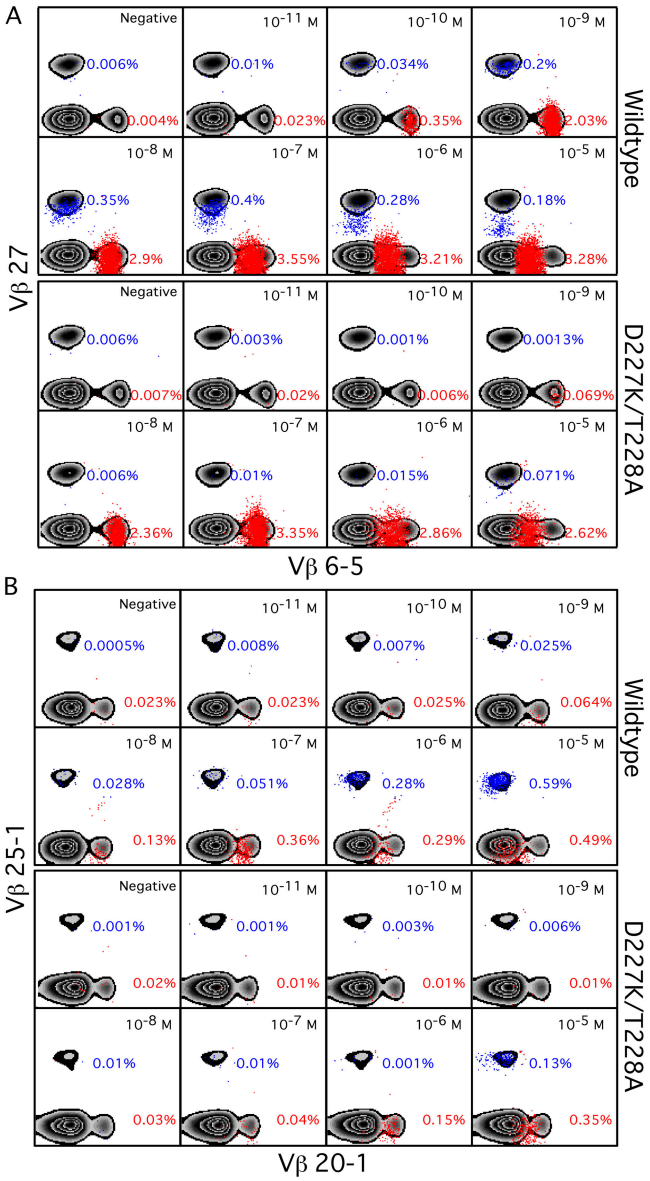

Figure 5. Functional titration experiments in the absence of pMHC-CD8 binding expose a proportionately greater coreceptor contribution to antigen sensitivity in low avidity clonotypes directly ex vivo. C1R cells expressing equivalent levels of either wild-type or CD8-null HLA A*0201 on the cell surface were pulsed with the indicated concentrations of either CMV NV9 (A) or EBV GL9 (B) peptide for 2 h and washed thoroughly. PBMCs from donor F (A) or donor T (B) were pulsed with the unrelated HLA A*0201-restricted peptide SLYNTVATL to block autologous presentation of NV9 or GL9 peptides, respectively. For each condition, 2×10^6 PBMCs were added to 10^6 C1R cells and incubated for 6 h in the presence of brefeldin A; cells were then analyzed for intracellular IFNγ production by flow cytometry (representative plots are shown in Fig. S1, available at http://www.jem.org/cgi/content/full/jem.20051357/DC1). Plots are gated on $CD3^+$, $CD8^+$ lymphocytes. Colored dots represent T cells expressing the indicated subdominant (blue) or dominant (red) TCRVβ that produce IFNγ; these events are superimposed on density plots representing the total $CD8^+$ T cell population according to expression of subdominant (y axis) or dominant (x axis) TCRVβ. The percentage of all $CD8^+$ T cells that express subdominant (blue) or dominant (red) TCRVβ and produce IFNγ is indicated. Precise quantification of the dominant clonotype, but not the subdominant clonotype, in B was hampered by TCR down-regulation. Peptide concentrations are shown at top right in each plot. Negative controls were mock-pulsed with medium. Other effector functions showed similar patterns (not depicted).

Table I. Antigen-specific uptake of GFP-labelled pMHCI complexes from the surface of C1R target cells

			HLA A*0201 heavy chain	
Antigen	TCRVβ	IFNγ[a]	Wild type[b]	D227K/T228A[b]
CMV-NV9	6-5	+	4.5	8.9
		−	1.7	3.0
	27	+	1.3	1.7
		−	0.8	1.3
EBV-GL9	20-1	+	9.6	16.4
		−	3.3	2.6
	25-1	+	4.8	11.2
		−	1.7	3.0

[a]$CD8^+$ T cells that do not secrete IFNγ in response to stimulation (−) represent the internal negative control for each assay.
[b]Values represent the percentage of $CD8^+$ T cells that contain GFP for each experimental condition.

impair the antigen-mediated triggering process (6, 31). We sought to confirm this with a direct examination of antigen uptake. Previous studies have demonstrated that $CD8^+$ T cells can internalize pMHCI complexes presented on the target cell surface (32, 33). To quantify this process at the level of individual antigen-specific clonotypes, we measured the frequency of GFP-expressing cells in each of the responding TCRVβ-defined $CD8^+$ T cell populations shown in Fig. 5 at the maximum peptide concentration. In all cases, the dominant clonotype displaying IFNγ production in response to cognate antigen-bearing targets acquired GFP more efficiently than the corresponding subdominant clonotype (Table I). These findings indicate that dominant antigen-specific $CD8^+$ T cell clonotypes internalize pMHCI complexes more efficiently than subdominant clonotypes when presented simultaneously with identical antigen-bearing target cells, and are consistent with the notion of avidity-based competitive signal extinction as a mechanism for clonal dominance (6).

In sum, these results substantiate the avidity profiles determined by physical analyses with soluble antigens (Figs. 3 and 4) and are consistent with a proportionately greater role for CD8 in the facilitation of antigen recognition by clonotypes with lower avidities (34).

Phenotypic properties of virus-specific $CD8^+$ T cell clonotypes directly ex vivo

If competition for cognate antigen is a substantial formative influence in vivo, then this phenomenon might become manifest as interclonal differences in maturation phenotype. To test this possibility, we conducted a phenotypic analysis of individual clonotypes contained within the $CD8^+$ T cell populations spe-

Published November 14, 2005

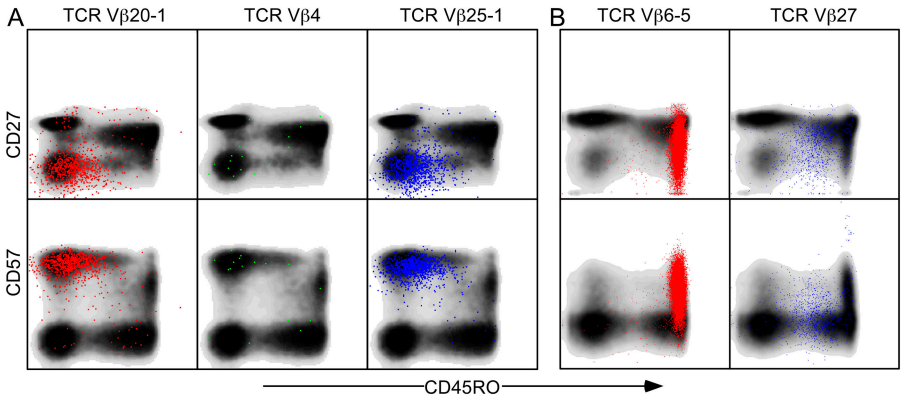

Figure 6. CD8+ T cell clonotypes specific for the same viral antigen can have similar or different memory phenotypes. PBMCs were stained with the cognate wild-type pMHCI tetramer and mAbs specific for CD8, CD27, CD45RO, CD57, and the indicated TCRVβ. The memory phenotype of the total CD8+ population is depicted as a black density plot, and the antigen-specific cells separated according to TCRVβ expression are shown superimposed as colored dots. (A) Distinct CD8+ T cell clonotypes specific for EBV GL9 in donor T exhibit similar memory phenotypes despite differences in avidity. (B) Distinct CD8+ T cell clonotypes specific for CMV NV9 in donor F exhibit different memory phenotypes.

cific for EBV GL9 in donor T and CMV NV9 in donor F using polychromatic flow cytometry (Fig. 6). For these experiments, only the relevant wild-type tetramers were used in conjunction with TCR Vβ-specific monoclonal antibodies to distinguish each antigen-specific clonotype; this approach standardizes the experimental conditions and obviates any biological anomalies that might be induced by reagents with differential CD8 binding properties. In donor T, dominant and subdominant clonotypes specific for EBV GL9 displayed almost identical terminally differentiated ($CD27^{-}CD45RO^{-}CD57^{+}$) phenotypes (Fig. 6 A); this relatively unusual phenotype suggests an ongoing response to active viral replication (35). Interestingly, however, when the light scatter profile was adjusted to incorporate larger and more granular cells, a distinct subpopulation of $CD3^{dim}CD8^{dim}CD57^{-}TCRV\beta20\text{-}1^{+}$ antigen-specific T cells was identified with the EBV GL9 tetramer after doublet exclusion; this is consistent with preferential antigen-derived signal sequestration by this clonotype even in the presence of a pMHCI–CD8 interaction (unpublished data). Terminally differentiated phenotypes also dominated the CMV- and EBV-specific CD8+ T cell populations in other donors (unpublished data). In donor F, however, clear interclonal phenotypic differences were observed in the CD8+ T cell population specific for CMV NV9. The dominant clonotype was terminally differentiated as defined by the expression of CD57 on the cell surface; the principal subdominant clonotype, in contrast, exhibited a less differentiated $CD45RO^{dim}CD57^{-}$ effector phenotype (Fig. 6 B). Thus, avidity differences can be reflected in cellular differentiation phenotype, with high avidity clonotypes preferentially driven toward replicative senescence.

Functional properties of virus-specific CD8+ T cells clonotypes directly ex vivo

To determine whether interclonal avidity differences are associated with functional heterogeneity in the CD8+ T cell response to cognate antigen, we developed a flow cytometric panel that enables the independent assessment of five distinct effector functions simultaneously at the single cell level. In donor F, the functional profile of the antigen-specific CD8+ T cell population in response to exogenous CMV NV9 peptide was dominated by 4/32 possible permutations defined on the basis of individual effector readouts; both the dominant and subdominant clonotypes, differentiated on the basis of their distinct phenotypic profiles, were equally distributed in each of these subsets (Fig. 7). Thus, although the nature of the CD8+ T cell response in the presence of saturating concentrations of exogenous peptide is not necessarily reflective of the in vivo situation, these results do demonstrate that clonotypes with different avidities for cognate antigen can mediate identical effector functions in the presence of a sufficient stimulus. This constitutes an important control and is consistent with the concept that interclonal differences in the strength of the antigen-derived signal, which can contribute to overall T cell fitness (36), occur at the limiting concentrations of antigen that are likely to be encountered in vivo and are not representative of inherent differences between T cell clonotypes.

DISCUSSION

In this study, we used a combination of point-mutated pMHCI antigens in both soluble and cell-associated forms, a modified template-switch anchored RT-PCR that detects all expressed *TCRBV* genes without bias, and polychromatic flow cytometric analysis of cellular function and phenotype to dissect directly ex vivo factors that contribute to the clonal structure of antigen-specific CD8+ T cell populations during persistent infection with CMV and EBV. A number of consistent features emerged from this analysis.

First, CD8+ T populations specific for CMV NV9 and EBV GL9 are oligoclonal and generally dominated by one or two prevalent clonotypes (Fig. 1, A and B). Furthermore, no consistent TCRBV CDR3 motifs were apparent in either

Published November 14, 2005

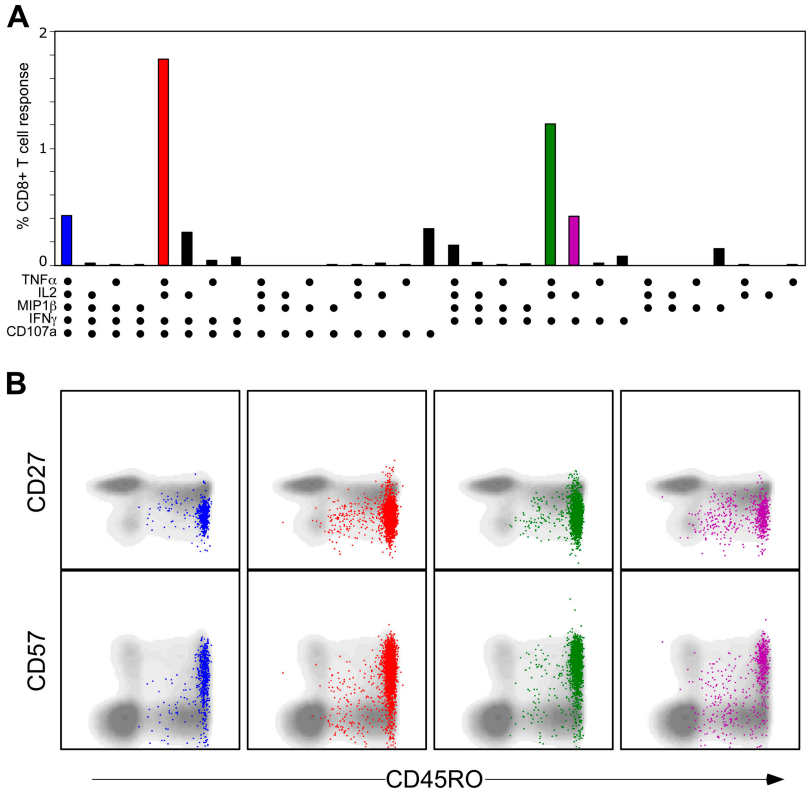

Figure 7. Individual CD8⁺ T cell clonotypes specific for the same antigen can display similar functionality despite differences in phenotype and avidity. (A) PBMCs from donor F were stimulated for 5 h with CMV NV9 peptide and stained with a panel of mAbs to examine degranulation (CD107a), cytokine production (IFNγ, TNFα, IL2), and chemokine production (MIP1β). The 31 possible positive responses that can be discerned from simultaneous examination of these five functional parameters are shown on the x axis. The total frequency of CD8⁺ T cells displaying each particular functional profile is shown on the y axis. The four major responses are colored in blue, red, green, and purple. (B) The memory phenotypes of specific T cells expressing one of the four major functional patterns shown in A are overlaid on the phenotype of the total CD8⁺ T cell population. Two memory populations are apparent for each functional response, corresponding directly to the phenotypes of the two major CD8⁺ T cell clonotypes specific for CMV NV9 (Fig. 6). All events shown are CD3⁺, CD8⁺, CD4⁻, CD14⁻, CD19⁻, with a small lymphocyte forward/side scatter profile excluding doublets and aggregates.

case. Thus, in contrast with some immunodominant CD8⁺ T cell responses, the peripheral TCR repertoire that can serve as a reservoir for recruitment of antigen-specific clonotypes is diverse and does not appear to be limited by the exacting structural constraints that can be imperative for functional pMHCI engagement (20). The potential for a given pMHCI complex to be recognized by TCRs with diverse structural features is likely to be a prerequisite for the occurrence of interclonal competition within an antigen-specific CD8⁺ T cell response.

Second, common antigen-specific clonotypes were observed in different individuals for each of the CMV- and EBV-specific CD8⁺ T cell populations (Fig. 1, A and B). Importantly, these public clonotypes were encoded distinctly at the nucleotide level in different donors and were confined by antigen specificity (Fig. 1 C). In addition, several recurrent patterns were observed at the level of primary TCRB CDR3 structure in the private repertoire specific for each antigen. These data provide evidence that cognate TCR selection in the periphery operates at the protein level as previously described for antibody responses, and implies that ongoing selection for optimal fit guides convergent clonal evolution in vivo.

Third, CD8⁺ T cells specific for CMV NV9 were characterized by high levels of avidity for cognate antigen in all donors tested (Figs. 2 A and 4; not depicted). This property is consistent with ongoing competition for antigen in vivo. Curiously, the same did not appear to hold for CD8⁺ T cells specific for EBV GL9, which exhibited comparatively greater dependency on the pMHCI–CD8 interaction for stable binding and uptake of soluble tetrameric antigen complexes (Figs. 2 B and 3; not depicted) and for activation (Fig. 5). Although the relationship between antigen avidity and affinity is complex, it seems feasible that these EBV-specific CD8⁺ T cells exhibit weaker TCR–pMHCI interaction affinities. There are several potential explanations for this observation. For example, it is known that high avidity CD8⁺ T cells are susceptible to apoptosis and clonal deletion under conditions of excess antigen load (37–39). This process contributes to the pattern and quality of the CD8⁺ T cell re-

Published November 14, 2005

sponse to persistent viral infections that evolves over time (40). Thus, it is reasonable to postulate that high levels of viremia during the acute phase of EBV infection might lead to a predominantly low avidity $CD8^+$ T cell response during the chronic phase, especially given that GL9 is a lytic epitope preferentially expressed in the early stages. In contrast, the early period of viral dissemination during CMV infection might be associated with fewer negative effects on the reactive immune repertoire, thereby allowing the continuous selection and accrual of high avidity clonotypes during the chronic phase of infection (41, 42). Further studies will be needed to distinguish whether the observed differences in $CD8^+$ T cell avidity for CMV- and EBV-derived epitopes reflect a function of virus biology or an intrinsic property of the epitopes themselves.

Fourth, clonal dominance within the hierarchical structure of $CD8^+$ T cell populations specific for CMV NV9 and EBV GL9 is a function of avidity for antigen. Thus, dominant clonotypes exhibited high levels of avidity directly ex vivo coupled to more sensitive functional response profiles, whereas the inverse applied to subdominant clonotypes (Figs. 3–5). These data provide evidence that interclonal competition for antigen is a formative influence during the maintenance of $CD8^+$ T cell populations specific for persistent DNA viruses. In addition, this process can be reflected by interclonal phenotypic dissociations, with high avidity clonotypes preferentially driven toward senescence presumably as a consequence of successful antigen sequestration (Fig. 6). This latter point is reinforced by the finding that $CD8^+$ T cell clonotypes with identical specificities can be equivalent in terms of their potential to respond functionally when presented with sufficient densities of cognate antigen (Fig. 7). Studies in murine models indicate that the sensitivity with which specific T cell populations recognize antigen can evolve during the development of an effector response independent of changes in TCR usage; the mechanisms involved include changes in membrane composition and the basal phosphorylation status of signaling molecules, and altered topographical organization of TCR and coreceptor (43–47). There is also some evidence for avidity maturation within antigen-specific T cell populations due to positive selection of cognate TCRs with both optimal affinity for pMHC and slower dissociation kinetics resulting in longer dwell times (8, 9, 12). In the present study, the observation that intrinsic avidity properties cosegregate with distinct clonotypes suggests that TCR-dependent mechanisms are the principal determinants of response optimization during antigen-driven $CD8^+$ T cell expansion in chronic infection. Although the relationship between antigen avidity and functional sensitivity is nonlinear, such progressive evolution toward high avidity $CD8^+$ T cell usage within the confines of peripheral T cell repertoire is potentially advantageous in terms of improved effector function delivery and control of viral replication (48–50).

Fifth, the data indicate that the differential compensatory role of CD8 enables the recruitment and maintenance of low avidity clonotypes within the antigen-specific $CD8^+$ T cell response, albeit at mostly subdominant frequencies, as suggested previously by studies of clones derived in vitro (27, 51). Indeed, it is apparent that this process, which affects both overall avidity and functional sensitivity in a manner dependent on CD8 expression levels and other variables (29), can enable low avidity clonotypes to coexist quite competitively in some instances with their higher avidity associates (Figs. 1, 3, and 5). Such coreceptor-mediated effects could serve to promote clonotypic diversity within antigen-experienced memory T cell pools and confer potential evolutionary advantages in the face of pathogens with variable antigenicity (21). Interestingly, a recent study concluded that an affinity threshold mechanism operates during the peripheral selection and expansion of antigen-specific $CD4^+$ T cell populations to limit the competitive advantage of clonotypes with the highest avidity and prevent monopolization of the response (12). It is possible that these distinct mechanisms for engendering clonotypic diversity reflect differences in the biophysical properties of the corresponding T cell coreceptors; thus, whereas CD8 has been shown to stabilize TCR–pMHCI complexes at the cell surface (52), the affinity of the pMHCII–CD4 interaction is substantially lower. Presumably, there is also a threshold in $CD8^+$ T cell populations beyond which further increases in avidity either fail to confer any additional competitive advantage or actually become deleterious. The present study does not examine these issues, but it seems likely that such a threshold might occur to limit peripheral antigen-driven selection when the optimal activation window is exceeded by clonotypes with excessively high avidity that escape thymic editing; under these circumstances, clonotypes with lower avidities might become dominant. Other scenarios can also be envisaged in which low avidity clonotypes might predominate. For example, a cross-reactive clonotype driven to proliferate by high avidity recognition of the true cognate antigen might be detected with wild-type pMHCI tetrameric complexes bearing the partial agonist peptide due to the compensatory capacity of the CD8 coreceptor. Further work is required to dissect these complex relationships that are created by the existence of antigen-specific $CD8^+$ T cells in the setting of a complex and dynamic system rather than in isolation.

Many different selection forces can potentially interact to define the clonotypic structure of a T cell population activated in response to a specific antigen. These formative processes include antigen-induced apoptosis, avidity-mediated competition, precursor frequency, senescence and exhaustion, and structural constraints (2–13, 20, 21, 37–39, 53). The relative impact of each of these factors under any given circumstance will likely vary according to the nature and dose of antigen, the duration of exposure, and the conditions under which it is encountered. In this study, we provide direct ex vivo evidence that competitive effects operate within $CD8^+$ T cell populations specific for epitopes derived from persistent DNA viruses to generate hierarchies that are dominated by clonotypes with high avidity for antigen during

Published November 14, 2005

human infection; concurrently, compensatory mechanisms mediated through the CD8 coreceptor act to mitigate this competitive advantage. These coincident processes likely serve to optimize the delivery of antiviral effector function while maintaining clonotypic diversity within the reactive memory T cell pool.

MATERIALS AND METHODS

Donors. Peripheral blood samples were obtained by apheresis from healthy volunteers and HIV-infected donors, selected according to CMV/EBV serostatus and HLA genotype, with appropriate Institutional Review Board approval. Donors D, H, K, R, S, and T were coinfected with HIV-1. Plasma virus load (copies HIV RNA/ml)/total $CD4^+$ T cell count (cells/μl blood) measurements at the time of study were: <50/1,329; 2,473/616; 25,902/502; <50/958; 261/937; and 3,198/452, respectively.

Peptides. The immunodominant HLA A*0201-restricted CMV and EBV epitopes used in this study are derived from the pp65 (NLVPMVATV; residues 495–503) and BMLFI (GLCTLVAML; residues 259–267) proteins, respectively. The corresponding peptides were synthesized to >95% purity (BioSynthesis).

Tetrameric pMHCI complexes. Tetrameric recombinant pMHCI antigens were produced as described previously (54). In brief, biotin-tagged HLA-A*0201 heavy chains and mutants thereof were expressed under the control of a T7 promoter as insoluble inclusion bodies in *Escherichia coli* strain BL21(DE3)pLysS (Novagen). IPTG-induced *E. coli* were lysed by repeated freeze/thaw cycles to release inclusion bodies that were subsequently purified by washing with a 0.5% Triton X-100 buffer (Sigma-Aldrich). The compound D227K/T228A mutation in the α3 domain of HLA A*0201 has been shown to abrogate CD8 binding without affecting the biophysical properties of the TCR docking platform (30). HLA A*0201 heavy chain and β_2m inclusion body preparations were denatured separately in 8 M of urea buffer (Sigma-Aldrich) and mixed at a 1:1 molar ratio; pMHCI was refolded in 2-mercaptoethylamine/cystamine (Sigma-Aldrich) redox buffer with the appropriate synthetic peptide (BioSynthesis). After buffer exchange into 10 mM Tris, pH 8.1, refolded monomer was purified by anion exchange. Purified monomers were biotinylated using d-biotin (Sigma-Aldrich) and BirA enzyme. Excess biotin was removed by gel filtration. Biotinylated pMHCI monomers were conjugated by addition of fluorochrome-conjugated streptavidin at a 4:1 molar ratio, respectively, to produce tetrameric pMHCI complexes. All pMHCI tetramers were freshly prepared for each experiment from pMHCI monomers stored at −80°C to avoid effects due to differences in protein stability (54). The concentration of tetramer as expressed throughout this work refers to the pMHCI component and was standardized for each comparative experiment. Once prepared, tetramers were stored in the dark at 4°C. Tetramer stains were performed at 37°C for 20 min as described previously (26). For competition assays, protease inhibitor mixes were excluded from the tetramer preparations.

Antibodies. Directly conjugated mAbs specific for the antigens listed were used in the following fluorochrome combinations available from commercial sources: (a) IL-2–allophycocyanin (APC); CD3-Cy7APC, IFNγ-FITC, MIP1β-PE, CD57-FITC, IFNγ-Cy7PE, and TNFα-Cy7PE (BD Biosciences); (b) CD4-Cy5.5PE (Caltag); (c) CD45RO-Texas red–PE (TRPE) and TCR Vβ-PE (Beckman Coulter). The following mAbs were conjugated in our laboratory according to standard protocols: CD4–cascade blue, CD14-Cy5PE, CD19-Cy5PE, CD27–cascade blue, CD107a-Alexa 680, CD8-quantum dot (Qdot) 655, CD8-Qdot 705, CD57-Qdot 565, and TCR Vβ-APC. Unconjugated mAbs were obtained from BD Biosciences (CD4, CD14, CD19, CD107a, CD8, CD57) or Beckman Coulter (TCR Vβ). Fluorochromes were obtained from the following vendors: (a) cascade blue and Alexa 680 (Invitrogen); (b) Cy5 (GE Healthcare); (c) APC (ProZyme); and (d) Qdot 565, Qdot 655, and Qdot 705 (Quantum Dot Corp.).

Cell culture. All experiments were performed directly ex vivo on fresh or frozen PBMCs isolated by standard Ficoll-Hypaque density gradient centrifugation (GE Healthcare). Cryopreserved samples were thawed rapidly and recovered overnight at 37°C/5% CO_2 in RPMI 1640 medium supplemented with 10% heat-inactivated FCS, 100 U/ml penicillin, 100 μg/ml streptomycin, and 2 mM L-glutamine (R10) before use. C1R cells expressing GFP-tagged, full-length wild-type HLA A*0201 and mutant D227K/T228A HLA A*0201 were produced according to previously described protocols (30).

Functional analysis of memory T cells. Purified PBMCs were adjusted to 10^6 cells/ml in R10. After addition of anti-CD28 and anti-CD49d costimulatory antibodies (1 μg/ml each; BD Biosciences), 0.7 μg/ml monensin (BD Biosciences), 10 μg/ml brefeldin A (Sigma-Aldrich), and pretitred anti-CD107a mAb conjugated to Alexa 680, 1 ml of the cell suspension was used for each experimental condition. Peptides were used at a final concentration of 2 μM. Negative controls that contained no added peptide, and positive controls that contained *Staphylococcus* enterotoxin B (Sigma-Aldrich) at 1 μg/ml were included in parallel for each assay. Cells were incubated for 5 h at 37°C/5% CO_2, washed once (1% bovine serum albumin/0.1% sodium azide in PBS), and stained with directly conjugated mAbs specific for the cell surface antigens CD4, CD8, CD14, CD19, CD27, CD45RO, and CD57 for 20 min in the dark at room temperature. After a further wash, cells were permeabilized using the Cytofix/Cytoperm kit (BD Biosciences) according to the manufacturer's instructions. After permeabilization, the cells were washed twice in the supplied buffer, and then stained with mAbs specific for CD3, IFNγ, MIP1β, TNFα, and IL-2 for 20 min in the dark at room temperature. Cells were washed one further time and fixed in PBS containing 1% paraformaldehyde.

Flow cytometry and cell sorting. Six-parameter analysis was conducted using a FACSCalibur flow cytometer (BD Immunocytometry Systems). Polychromatic analysis of phenotype and function was performed using a modified LSR II flow cytometer (BD Immunocytometry Systems), equipped for the detection of 17 fluorescent parameters. A minimum of 750,000 total events was collected for each sample. Data analysis was performed in all cases using FlowJo version 6.0 (TreeStar Inc.). Cells stained for analysis of clonotype composition were sorted at 25 PSI using a modified FACS DIVA (Becton Dickinson). Instrument set-up was performed according to the manufacturer's instructions. Electronic compensation was conducted with antibody-capture beads (BD Biosciences) stained separately with individual mAbs used in the test samples. Post-sort purity was consistently >99%.

Clonotype analysis. The relevant antigen-specific $CD8^+$ T cell populations were sorted directly into 1.5 ml microtubes containing 100 μl RNAlater (Ambion Inc.). For the purposes of this study, clonotype analysis was performed only on cells labeled physically with cognate pMHCI tetramers; capture assays based on biological readouts potentially misrepresent the repertoire due to functional impairment of $CD8^+$ T cells during persistent viral infections. At least 5,000 cells were collected for each experimental condition. After cell lysis, mRNA was extracted (Oligotex Kit; QIAGEN) and subjected to a nonnested, template-switch anchored RT-PCR using a 3′ TCRB constant region primer (5′-GCTTCTGATGGCTCAAACACAGCGACCTC-3′) as described previously (18). Amplified products were ligated into pGEM-T Easy vector (Promega) and cloned by transformation of competent DH5α *E. coli*. Selected colonies were amplified by PCR using standard M13 primers and then sequenced from an insert-specific primer using fluorescent dye terminator chemistry (Applied Biosystems). A minimum of 50 clones was generated and analyzed per sample. Dominant and subdominant assignments as used in this work refer to clonotype prevalence, which is accurately reproduced by the molecular method described. Pseudogenes and "nonfunctional" sequences that could not be resolved after inspection of the individual chromatograms were discarded from the analysis. Nucleotide comparisons were used to establish clonal identity. Data analysis was performed using Sequencher Version 4.2 (Gene Codes Corporation). The IMGT nomenclature system is used throughout this work (55).

Online supplemental material. Fig. S1 shows representative intracellular IFNγ plots and the gating strategy used to generate Fig. 5. Online supplemental material is available at http://www.jem.org/cgi/content/full/jem.20051357/DC1.

We thank D. Ambrozak for cell sorting.

D.A. Price is a Medical Research Council (UK) Clinician Scientist.

The authors have no conflicting financial interests.

Submitted: 7 July 2005
Accepted: 19 September 2005

REFERENCES

1. van der Merwe, P.A., and S.J. Davis. 2003. Molecular interactions mediating T cell antigen recognition. *Annu. Rev. Immunol.* 21:659–684.
2. Kedl, R.M., J.W. Kappler, and P. Marrack. 2003. Epitope dominance, competition and T cell affinity maturation. *Curr. Opin. Immunol.* 15: 120–127.
3. Butz, E.A., and M.J. Bevan. 1998. Massive expansion of antigen-specific $CD8^+$ T cells during an acute virus infection. *Immunity.* 8:167–175.
4. Smith, A.L., M.E. Wikstrom, and B. Fazekas de St Groth. 2000. Visualizing T cell competition for peptide/MHC complexes: a specific mechanism to minimize the effect of precursor frequency. *Immunity.* 13:783–794.
5. Kedl, R.M., W.A. Rees, D.A. Hildeman, B. Schaefer, T. Mitchell, J. Kappler, and P. Marrack. 2000. T cells compete for access to antigen-bearing antigen-presenting cells. *J. Exp. Med.* 192:1105–1113.
6. Kedl, R.M., B.C. Schaefer, J.W. Kappler, and P. Marrack. 2002. T cells down-modulate peptide-MHC complexes on APCs in vivo. *Nat. Immunol.* 3:27–32.
7. McHeyzer-Williams, M.G., and M.M. Davis. 1995. Antigen-specific development of primary and memory T cells in vivo. *Science.* 268:106–111.
8. Savage, P.A., J.J. Boniface, and M.M. Davis. 1999. A kinetic basis for T cell receptor repertoire selection during an immune response. *Immunity.* 10:485–492.
9. Busch, D.H., and E.G. Pamer. 1999. T cell affinity maturation by selective expansion during infection. *J. Exp. Med.* 189:701–710.
10. Rees, W., J. Bender, T.K. Teague, R.M. Kedl, F. Crawford, P. Marrack, and J. Kappler. 1999. An inverse relationship between T cell receptor affinity and antigen dose during CD4(+) T cell responses in vivo and in vitro. *Proc. Natl. Acad. Sci. USA.* 96:9781–9786.
11. Lanzavecchia, A. 2002. Lack of fair play in the T cell response. *Nat. Immunol.* 3:9–10.
12. Malherbe, L., C. Hausl, L. Teyton, and M.G. McHeyzer-Williams. 2004. Clonal selection of helper T cells is determined by an affinity threshold with no further skewing of TCR binding properties. *Immunity.* 21:669–679.
13. Bousso, P., A. Casrouge, J.D. Altman, M. Haury, J. Kanellopoulos, J.P. Abastado, and P. Kourilsky. 1998. Individual variations in the murine T cell response to a specific peptide reflect variability in naive repertoires. *Immunity.* 9:169–178.
14. De Boer, R.J., and A.S. Perelson. 1994. T cell repertoires and competitive exclusion. *J. Theor. Biol.* 169:375–390.
15. Wolpert, E.Z., P. Grufman, J.K. Sandberg, A. Tegnesjo, and K. Karre. 1998. Immunodominance in the CTL response against minor histocompatibility antigens: interference between responding T cells, rather than with presentation of epitopes. *J. Immunol.* 161:4499–4505.
16. Grufman, P., E.Z. Wolpert, J.K. Sandberg, and K. Karre. 1999. T cell competition for the antigen-presenting cell as a model for immunodominance in the cytotoxic T lymphocyte response against minor histocompatibility antigens. *Eur. J. Immunol.* 29:2197–2204.
17. Riddell, S.R., and P.D. Greenberg. 1995. Principles for adoptive T cell therapy of human viral diseases. *Annu. Rev. Immunol.* 13:545–586.
18. Douek, D.C., M.R. Betts, J.M. Brenchley, B.J. Hill, D.R. Ambrozak, K.L. Ngai, N.J. Karandikar, J.P. Casazza, and R.A. Koup. 2002. A novel approach to the analysis of specificity, clonality, and frequency of HIV-specific T cell responses reveals a potential mechanism for control of viral escape. *J. Immunol.* 168:3099–3104.
19. Kjer-Nielsen, L., C.S. Clements, A.W. Purcell, A.G. Brooks, J.C. Whisstock, S.R. Burrows, J. McCluskey, and J. Rossjohn. 2003. A structural basis for the selection of dominant αβ T cell receptors in antiviral immunity. *Immunity.* 18:53–64.
20. Stewart-Jones, G.B., A.J. McMichael, J.I. Bell, D.I. Stuart, and E.Y. Jones. 2003. A structural basis for immunodominant human T cell receptor recognition. *Nat. Immunol.* 4:657–663.
21. Price, D.A., S.M. West, M.R. Betts, L.E. Ruff, J.M. Brenchley, D.R. Ambrozak, Y. Edghill-Smith, M.J. Kuroda, D. Bogdan, K. Kunstman, et al. 2004. T cell receptor recognition motifs govern immune escape patterns in acute SIV infection. *Immunity.* 21:793–803.
22. Lim, A., L. Trautmann, M.A. Peyrat, C. Couedel, F. Davodeau, F. Romagne, P. Kourilsky, and M. Bonneville. 2000. Frequent contribution of T cell clonotypes with public TCR features to the chronic response against a dominant EBV-derived epitope: application to direct detection of their molecular imprint on the human peripheral T cell repertoire. *J. Immunol.* 165:2001–2011.
23. Pittet, M.J., V. Rubio-Godoy, G. Bioley, P. Guillaume, P. Batard, D. Speiser, I. Luescher, J.C. Cerottini, P. Romero, and A. Zippelius. 2003. α3 domain mutants of peptide/MHC class I multimers allow the selective isolation of high avidity tumor-reactive CD8 T cells. *J. Immunol.* 171:1844–1849.
24. Choi, E.M., J.L. Chen, L. Wooldridge, M. Salio, A. Lissina, N. Lissin, I.F. Hermans, J.D. Silk, F. Mirza, M.J. Palmowski, et al. 2003. High avidity antigen-specific CTL identified by CD8-independent tetramer staining. *J. Immunol.* 171:5116–5123.
25. Bodinier, M., M.A. Peyrat, C. Tournay, F. Davodeau, F. Romagne, M. Bonneville, and F. Lang. 2000. Efficient detection and immunomagnetic sorting of specific T cells using multimers of MHC class I and peptide with reduced CD8 binding. *Nat. Med.* 6:707–710.
26. Whelan, J.A., P.R. Dunbar, D.A. Price, M.A. Purbhoo, F. Lechner, G.S. Ogg, G. Griffiths, R.E. Phillips, V. Cerundolo, and A.K. Sewell. 1999. Specificity of CTL interactions with peptide-MHC class I tetrameric complexes is temperature dependent. *J. Immunol.* 163:4342–4348.
27. Couedel, C., M. Bodinier, M.A. Peyrat, M. Bonneville, F. Davodeau, and F. Lang. 1999. Selection and long-term persistence of reactive CTL clones during an EBV chronic response are determined by avidity, CD8 variable contribution compensating for differences in TCR affinities. *J. Immunol.* 162:6351–6358.
28. Kerry, S.E., J. Buslepp, L.A. Cramer, R. Maile, L.L. Hensley, A.I. Nielsen, P. Kavathas, B.J. Vilen, E.J. Collins, and J.A. Frelinger. 2003. Interplay between TCR affinity and necessity of coreceptor ligation: high-affinity peptide-MHC/TCR interaction overcomes lack of CD8 engagement. *J. Immunol.* 171:4493–4503.
29. Maile, R., C.A. Siler, S.E. Kerry, K.E. Midkiff, E.J. Collins, and J.A. Frelinger. 2005. Peripheral "CD8 tuning" dynamically modulates the size and responsiveness of an antigen-specific T cell pool in vivo. *J. Immunol.* 174:619–627.
30. Purbhoo, M.A., J.M. Boulter, D.A. Price, A.L. Vuidepot, C.S. Hourigan, P.R. Dunbar, K. Olson, S.J. Dawson, R.E. Phillips, B.K. Jakobsen, et al. 2001. The human CD8 coreceptor effects cytotoxic T cell activation and antigen sensitivity primarily by mediating complete phosphorylation of the T cell receptor zeta chain. *J. Biol. Chem.* 276: 32786–32792.
31. van Bergen, J., Y. Kooy, and F. Koning. 2001. CD4-independent T cells impair TCR triggering of CD4-dependent T cells: a putative mechanism for T cell affinity maturation. *Eur. J. Immunol.* 31:646–652.
32. Huang, J.F., Y. Yang, H. Sepulveda, W. Shi, I. Hwang, P.A. Peterson, M.R. Jackson, J. Sprent, and Z. Cai. 1999. TCR-mediated internalization of peptide-MHC complexes acquired by T cells. *Science.* 286:952–954.
33. Tomaru, U., Y. Yamano, M. Nagai, D. Maric, P.T. Kaumaya, W. Biddison, and S. Jacobson. 2003. Detection of virus-specific T cells and CD8(+) T-cell epitopes by acquisition of peptide-HLA-GFP complexes: analysis of T-cell phenotype and function in chronic viral infections. *Nat. Med.* 9:469–476.
34. Alexander, M.A., C.A. Damico, K.M. Wieties, T.H. Hansen, and J.M. Connolly. 1991. Correlation between CD8 dependency and determinant density using peptide-induced, Ld-restricted cytotoxic T lympho-

cytes. *J. Exp. Med.* 173:849–858.
35. Catalina, M.D., J.L. Sullivan, R.M. Brody, and K. Luzuriaga. 2002. Phenotypic and functional heterogeneity of EBV epitope-specific $CD8^+$ T cells. *J. Immunol.* 168:4184–4191.
36. Gett, A.V., F. Sallusto, A. Lanzavecchia, and J. Geginat. 2003. T cell fitness determined by signal strength. *Nat. Immunol.* 4:355–360.
37. Alexander-Miller, M.A., G.R. Leggatt, A. Sarin, and J.A. Berzofsky. 1996. Role of antigen, CD8, and cytotoxic T lymphocyte (CTL) avidity in high dose antigen induction of apoptosis of effector CTL. *J. Exp. Med.* 184:485–492.
38. Anderton, S.M., C.G. Radu, P.A. Lowrey, E.S. Ward, and D.C. Wraith. 2001. Negative selection during the peripheral immune response to antigen. *J. Exp. Med.* 193:1–11.
39. Derby, M.A., J.T. Snyder, R. Tse, M.A. Alexander-Miller, and J.A. Berzofsky. 2001. An abrupt and concordant initiation of apoptosis: antigen-dependent death of $CD8^+$ CTL. *Eur. J. Immunol.* 31:2951–2959.
40. Welsh, R.M., K. Bahl, and X.Z. Wang. 2004. Apoptosis and loss of virus-specific $CD8^+$ T-cell memory. *Curr. Opin. Immunol.* 16:271–276.
41. Lin, M.Y., and R.M. Welsh. 1998. Stability and diversity of T cell receptor repertoire usage during lymphocytic choriomeningitis virus infection of mice. *J. Exp. Med.* 188:1993–2005.
42. Karrer, U., S. Sierro, M. Wagner, A. Oxenius, H. Hengel, U.H. Koszinowski, R.E. Phillips, and P. Klenerman. 2003. Memory inflation: continuous accumulation of antiviral $CD8^+$ T cells over time. *J. Immunol.* 170:2022–2029.
43. Fahmy, T.M., J.G. Bieler, M. Edidin, and J.P. Schneck. 2001. Increased TCR avidity after T cell activation: a mechanism for sensing low-density antigen. *Immunity.* 14:135–143.
44. Hesse, M.D., A.Y. Karulin, B.O. Boehm, P.V. Lehmann, and M. Tary-Lehmann. 2001. A T cell clone's avidity is a function of its activation state. *J. Immunol.* 167:1353–1361.
45. Slifka, M.K., and J.L. Whitton. 2001. Functional avidity maturation of CD8(+) T cells without selection of higher affinity TCR. *Nat. Immunol.* 2:711–717.
46. Cawthon, A.G., and M.A. Alexander-Miller. 2002. Optimal colocalization of TCR and CD8 as a novel mechanism for the control of functional avidity. *J. Immunol.* 169:3492–3498.
47. Kersh, E.N., S.M. Kaech, T.M. Onami, M. Moran, E.J. Wherry, M.C. Miceli, and R. Ahmed. 2003. TCR signal transduction in antigen-specific memory CD8 T cells. *J. Immunol.* 170:5455–5463.
48. Alexander-Miller, M.A., G.R. Leggatt, and J.A. Berzofsky. 1996. Selective expansion of high- or low-avidity cytotoxic T lymphocytes and efficacy for adoptive immunotherapy. *Proc. Natl. Acad. Sci. USA.* 93:4102–4107.
49. Derby, M., M. Alexander-Miller, R. Tse, and J. Berzofsky. 2001. High-avidity CTL exploit two complementary mechanisms to provide better protection against viral infection than low-avidity CTL. *J. Immunol.* 166:1690–1697.
50. Sedlik, C., G. Dadaglio, M.F. Saron, E. Deriaud, M. Rojas, S.I. Casal, and C. Leclerc. 2000. In vivo induction of a high-avidity, high-frequency cytotoxic T-lymphocyte response is associated with antiviral protective immunity. *J. Virol.* 74:5769–5775.
51. Levitsky, V., P.O. de Campos-Lima, T. Frisan, and M.G. Masucci. 1998. The clonal composition of a peptide-specific oligoclonal CTL repertoire selected in response to persistent EBV infection is stable over time. *J. Immunol.* 161:594–601.
52. Wooldridge, L., H.A. van den Berg, M. Glick, E. Gostick, B. Laugel, S.L. Hutchinson, A. Milicic, J.M. Brenchley, D.C. Douek, D.A. Price, and A.K. Sewell. 2005. Interaction between the CD8 coreceptor and major histocompatibility complex class I stabilizes T cell receptor-antigen complexes at the cell surface. *J. Biol. Chem.* 280:27491–27501.
53. Davenport, M.P., C. Fazou, A.J. McMichael, and M.F. Callan. 2002. Clonal selection, clonal senescence, and clonal succession: the evolution of the T cell response to infection with a persistent virus. *J. Immunol.* 168:3309–3317.
54. Hutchinson, S.L., L. Wooldridge, S. Tafuro, B. Laugel, M. Glick, J.M. Boulter, B.K. Jakobsen, D.A. Price, and A.K. Sewell. 2003. The CD8 T cell coreceptor exhibits disproportionate biological activity at extremely low binding affinities. *J. Biol. Chem.* 278:24285–24293.
55. Lefranc, M.P., C. Pommie, M. Ruiz, V. Giudicelli, E. Foulquier, L. Truong, V. Thouvenin-Contet, and G. Lefranc. 2003. IMGT unique numbering for immunoglobulin and T cell receptor variable domains and Ig superfamily V-like domains. *Dev. Comp. Immunol.* 27:55–77.